









Article

Monitoring of Multi-Aspect Drought Severity and Socio-Economic Status in the Semi-Arid Regions of Eastern Tamil Nadu, India

Venkatesh Ravichandran ¹, Komali Kantamaneni ^{2,*}, Thilagaraj Periasamy ³, Priyadarsi D. Roy ⁴,
Jothiramalingam Killivalavan ³, Sajimol Sundar ⁵, Lakshumanan Chokkalingam ⁵
and Masilamani Palanisamy ³

- ¹ Department of Civil Engineering, Indian Institutes of Technology, Guwahati 781039, Assam, India; r.v@rnd.iitg.ac.in
- ² Faculty of Science and Technology, University of Central Lancashire, Preston PR1 2HE, UK
- ³ Department of Geography, School of Earth Science, Bharathidasan University, Tiruchirappalli 620024, Tamil Nadu, India; pthilagaraj23@gmail.com (T.P.); killivalavan@bdu.ac.in (J.K.); masilamani@bdu.ac.in (M.P.)
- ⁴ Instituto de Geología, Universidad Nacional Autónoma de México (UNAM), Ciudad Universitaria, Ciudad de México 04510, Mexico; roy@geologia.unam.mx
- ⁵ Department of Remote Sensing, School of Earth Science, Bharathidasan University, Tiruchirappalli 620023, Tamil Nadu, India; shamisaji17@gmail.com (S.S.); drlaks@bdu.ac.in (L.C.)
- * Correspondence: kkantamaneni@uclan.ac.uk



Citation: Ravichandran, V.; Kantamaneni, K.; Periasamy, T.; Roy, P.D.; Killivalavan, J.; Sundar, S.; Chokkalingam, L.; Palanisamy, M. Monitoring of Multi-Aspect Drought Severity and Socio-Economic Status in the Semi-Arid Regions of Eastern Tamil Nadu, India. *Water* **2022**, *14*, 2049. <https://doi.org/10.3390/w14132049>

Academic Editor: George Arhonditsis

Received: 29 May 2022

Accepted: 23 June 2022

Published: 27 June 2022

Publisher's Note: MDPI stays neutral with regard to jurisdictional claims in published maps and institutional affiliations.



Copyright: © 2022 by the authors. Licensee MDPI, Basel, Switzerland. This article is an open access article distributed under the terms and conditions of the Creative Commons Attribution (CC BY) license (<https://creativecommons.org/licenses/by/4.0/>).

Abstract: A framework was set up to monitor drought in the semi-arid regions of eastern Tamil Nadu, southern India, for the period of 2014–2018 CE with the application of the standardized precipitation index (SPI), the scaled drought-condition index (SDCI), and the standardized water-level index (SWI). The results emphasized that this region had a negative precipitation anomaly and vegetative stress, both of which triggered meteorological and agricultural droughts and caused significant losses in the farming sector. The distributions of extreme and high-level hydrological droughts were at their maximum in 2017 CE. The multi-drought severity index (MDSI), implemented to assess the combined impact and highlighting the gradient of affected areas, illustrated that the eastern region (i.e., Jayankondam block) was the most extremely affected, followed by the northern and southern regions (i.e., T.Palur and Andimadam), which were moderately affected by droughts. The extremely affected eastern region has less of an ability to overcome droughts due to its socio-economic vulnerability, with its greater population and household density leading to the over-exploitation of potential resources. Therefore, the focus of this study is on the monitoring of drought severity in micro-administrative units to suggest an appropriate management plan. Hence, the extreme-drought-prone block (Jayankondam) should be given high priority in monitoring and implementing long-term management practices for its conservation and resilience against the effects of severe droughts.

Keywords: multi-drought severity index; meteorological drought; agricultural drought; hydrological drought; Ariyalur; India

1. Introduction

Drought is one of the natural hazards that occur due to deficits in precipitation. It causes agricultural stress and affects the ecological environment, as well as the socio-economic conditions, in the arid and semi-arid regions of different parts of the world [1–5]. Furthermore, droughts cause water scarcity and a lack of food crops for populations [6]. The global warming of the modern era has enhanced the frequency of droughts [7–9]. However, it is difficult to monitor the spatial extent and temporal origin of these anthropogenic droughts [10]. The elements leading to droughts and the elements that are affected by droughts are interrelated [6,11]. Different aspects of drought are sensitive to precipitation,

humidity, and soil moisture and groundwater fluctuation [12,13]. Unusual rainfall patterns and substantial temperature anomalies affect vegetation and lead to groundwater stress, which contributes towards extreme droughts [13]. Lower rainfall profiles lead to a higher impact on groundwater and cause hydrological droughts [14,15]. Even though the deterministic prediction of drought severity is a challenging task, the availability of temporal data facilitates its continuous monitoring through the analysis of agricultural, meteorological, hydrological, and socio-economic droughts [16]. Meteorological and agricultural droughts create more vulnerability. Hence, the quantitative assessment of the regional patterns of droughts, their degree of concentration, and the spatial and temporal changes evolving from the indices are used to mitigate droughts in management approaches [17–19]. The effective management and consistent determination of drought with precise temporal monitoring and prediction also help policymakers to formulate new strategies for the sustainable development of natural resources [20,21].

In an agrarian country such as India, where agriculture is the backbone of GDP, around 16% of the total land is drought-prone [22]. Meteorological droughts in India are caused by a lack of monsoonal rainfall; these droughts may become more severe in the near future, affecting food crops, industrial development, and power generation [15,22]. The semi-arid regions in the eastern area of the Tamil Nadu state in southern India (i.e., Ariyalur) have been adversely affected due to climate change. It was noted in the field study that most of this region has vegetation stress, as well as scarce surface water and groundwater for domestic and irrigation purposes. Thus, the region needs a critical assessment of multi-aspect drought conditions and the continuous monitoring of triggering factors.

However, the majority of the studies on drought assessments hardly utilize the multiple remote-sensing datasets available across the globe, particularly in India. The framework of this study is formulated to overcome this limitation by adopting multiple satellite products and ancillary data for the assessment of multi-droughts at the micro-administrative level (i.e., Ariyalur), along with the area's socioeconomic status.

In this study, we proceeded with the application of satellite datasets, such as the multispectral Landsat Optical Land Imager (OLI) [23–25], measurements of monthly precipitation using the tropical rainfall measuring mission (TRMM 3B43) [2,26–29] and ancillary data on monthly precipitation [30–34] and groundwater levels [5,13,15,35]. The district census handbook (DCHB) and primary census abstract (PCA) of the Census 2011 data were used for assessing the socio-economic vulnerability [36–38]. Insights from previous research in different parts of the world helped to form the approach to the index-based drought monitoring and the demarcation of the drought-prone areas [5,6,15,18,22,25,39–43]. In the present study, we monitored the meteorological, agricultural, and hydrological droughts by using ancillary and multi-sensor remote sensing indices, such as the standardized precipitation index (SPI), the scaled drought-condition index (SDCI), and the standardized water-level index (SWI), with appropriate datasets for the period of 2014–2018 CE. In the meteorological drought analysis, the deficiencies in the precipitation and climatic anomalies were quantified through the standardized precipitation index (SPI) with the monthly rainfall data. The agricultural drought was computed through multi-sensor remote-sensing indices, such as the scaled drought-condition index (SDCI). The SDCI was evaluated with the integration of three significant indices: the precipitation-condition index (PCI), the temperature-condition index (TCI) and the vegetation-condition index (VCI). Thus, the proportion of the temperature stress (TCI), the precipitation deficit (PCI), and the irregularities in the vegetative growth (VCI) were combined to highlight the drought-prone agricultural regions. Next, the standardized water-level index (SWI) was used for hydrological drought monitoring. The SWI signified the quantity and distribution of the aquifer stress by utilizing the monthly groundwater level data. The multi-drought severity index (MDSI) was introduced in this study to evaluate the combined effect of the three drought types. The MDSI presents the severity of meteorological, agricultural, and hydrological droughts on a common intensity scale to identify the regions affected by severe multiple

droughts. The MDSI was computed with three subsequent indices of SPI, SDCI, and SWI, in which the empirical weights applied were 0.3, 0.4, and 0.3 respectively.

Thus, the aim of this study was to identify the overall drought-affected areas and the intensity of different drought conditions affecting the study region through the multi-drought severity index (MDSI). The findings were compared with the socio-economic factors to highlight the vulnerable blocks, which reveal the power of individuals and management to mitigate the effects of future occurrences.

2. Study Area

The Ariyalur district in the eastern part of Tamil Nadu state, in southern India, is situated beside the western Cauvery Delta agro-climatic zone (Figure 1a) ($11^{\circ}24'25''$ to $10^{\circ}52'14''$ N latitude and $78^{\circ}55'28''$ to $79^{\circ}29'57''$ E longitude). It covers an area of about 2038 km², bordered to the north by Cuddalore, to the south by Thanjavur, to the east by Thanjavur and Nagapattinam, and to the west by the Perambalur and Tiruchirapalli districts. This district comprises 3 administrative taluks (Ariyalur, Udayarpalayam, and Sendurai), 6 blocks (Andimadam, Ariyalur, Jayankondam, Sendurai, T.Palur, and Thirumanur), and 213 revenue villages. The geology comprises fossiliferous limestone, sandstone, clay, and marl, and the primary geomorphic structures are alluvial plain and buried pediments [44]. This region is also well known for its deposits of celeste, limestone, shale, sandstone, canker, and phosphate nodules. These materials are used as primary raw materials for cement manufacturing in eight different plants. The occurrence of lignite, oil, and gas pockets has been reported in the Udayarpalayam and Andimadam taluks. The study area has two river systems (i.e., the Vellar and Kollidam rivers) and it is characterized by a tropical climate, with an annual average precipitation of about 1139 mm and temperature of 29.6 °C. It has been classified as semi-arid by the Tamil Nadu government. The predominant soil types are red loamy soil and alluvium. The population, of about 752,481 individuals, has a density distribution of 389 persons per km², according to the 2011 census. We selected 11 continuous monitoring rain-gauge stations and 76 sample-well locations for monitoring the meteorological and hydrological droughts.

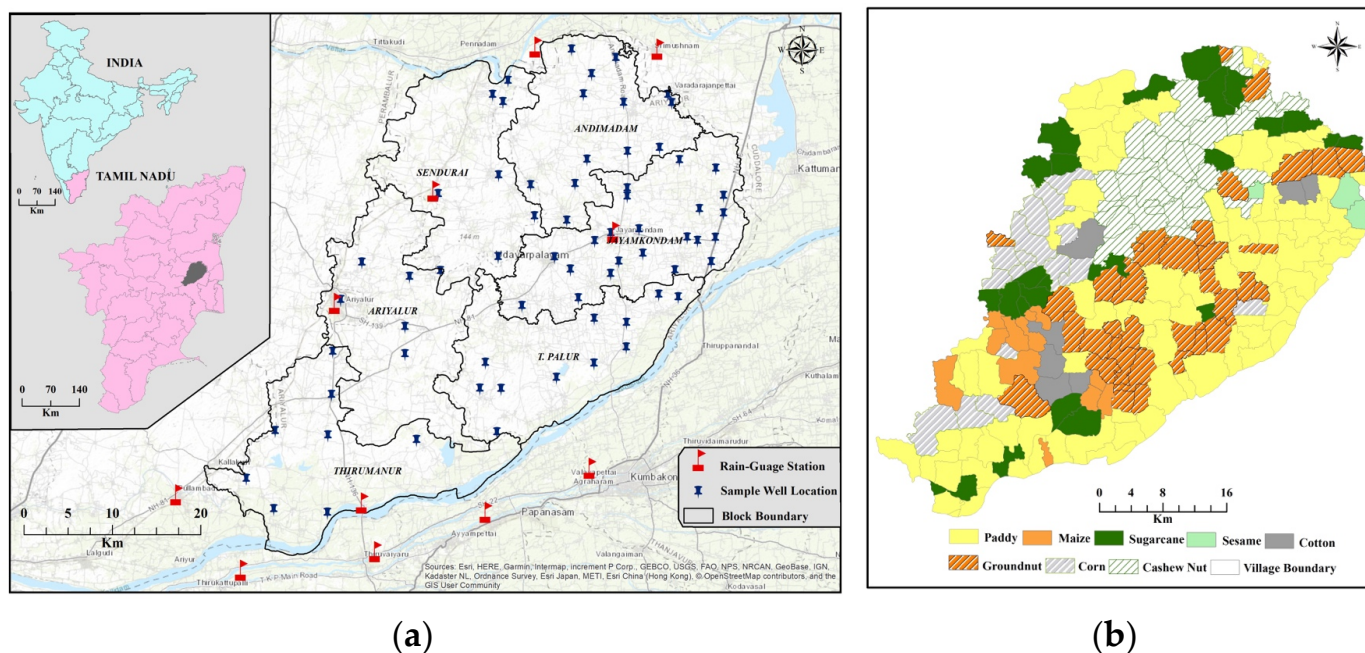


Figure 1. Map showing the locational information on the Ariyalur District in eastern Tamil Nadu (South India): (a) the distribution of rain-gauge stations and borewell locations; (b) spatial distribution of different crops cultivated in Ariyalur district of south India.

The spatial distribution of the cultivated crops was considered to estimate the total effect of the droughts on the food crops (Figure 1b). The major crops in the study area include paddy, cotton, corn, groundnut, maize, sugarcane, sesame, and cashew nut. Paddy is the most prominently cultivated crop, and it is distributed in the eastern and southern regions of the study area. Its distribution has a direct surge on the surface and groundwater stress in the entire region. The next most heavily cultivated crops, behind paddy, are corn, groundnut, and cashew nut, and the remaining crops are sparsely cultivated.

3. Materials and Methods

The assessment and monitoring of multi-aspect drought conditions were carried out with multiple datasets in a spatio-temporal dimension by calculating the standardized precipitation index (SPI) for evaluating meteorological drought, scaled drought-condition index (SDCI) for evaluating agricultural drought, and the standardized water-level index (SWI) for evaluating hydrological drought. The multi-dimensional drought assessment was carried out by introducing the new multi-drought severity index (MDSI), which processed all the drought indices (SPI, SDCI, and SWI) in a standard severity scale with the empirical weights of 0.3, 0.4, and 0.3, respectively. Both the ancillary and remote-sensing data covered the baseline period (2014–2018 CE) of temporal monitoring during the northeastern monsoon (October, November, and December) season (Table 1). The dataset comprised (i) daily precipitation, acquired through the continuous-monitoring rain-gauge station at the Regional Meteorological Center (RMC) in Chennai, (ii) multispectral imagery of Landsat 8 OLI (Optical Land Imager) from UGSG earth explorer, (iii) satellite-based monthly precipitation of TRMM 3B43 (tropical rainfall measuring mission), and (iv) monthly groundwater-level data from the public works department (PWD), Chennai. The results were compared with the socio-economic vulnerability, which was analyzed with the influencing factors of population density (PD), household density (HD), literacy ratio (LR), and working-population ratio (WPR). ArcMap 10.4 software was used for data processing and mapping and the detailed methodology was described in the in the Figure 2.

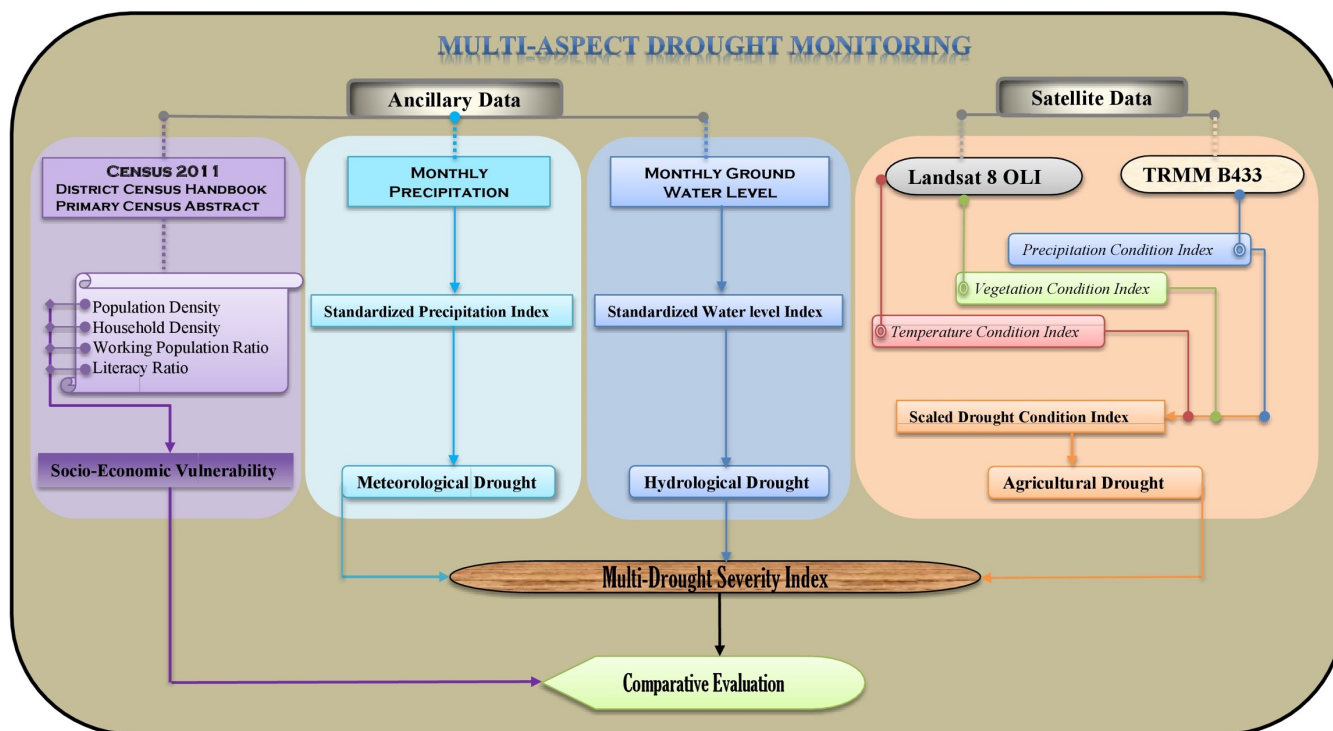


Figure 2. Methodological framework of multi-aspect drought-severity monitoring and assessment of socio-economic status in Ariyalur district of southern India.

Table 1. Description of the dataset used for this study of multi-aspect drought-severity monitoring and assessment.

S. No.	Data Sets	Variable	Period	Resolution	Source
1	Rainfall	SPI	1989–2018	–	RMC, Chennai
2	Landsat 8 OLI	NDVI, LST, VCI, TCI	2014–2018	30 m	Earth Explorer
3	TRMM 3B43	PCI	2014–2018	27 km	NASA Mirador
4	Ground Water Level	SWI	2004–2018	–	PWD, Chennai
5	Census	PD, HD, LR, WPR	2011	–	Census India

3.1. Meteorological Drought

Standardized precipitation index (SPI) is an index-based meteorological drought-severity monitoring method, and it is considered to be one of the most significant indices for monitoring meteorological-drought-affected regions [45,46]. It needs monthly precipitation data for 30 consecutive years. Here, we used the monthly precipitation data from 1989 to 2018 for computing SPI with the interval range of one month (SPI-1) using the formula in Table 2 [30]. The study period (2014–2018 CE) of northeastern monsoon season was extracted to map spatio-temporal distributions of drought severity.

3.2. Agricultural Drought

Precipitation-condition index (PCI) is a remote-sensing-based drought-monitoring technique that represents abnormalities in climatic signs and spatio-temporal deficits in precipitation [2,47,48]. We employed the satellite-based TRMM 3B43 monthly precipitation data in the analysis [49]. This global gridded dataset has a spatial resolution of $0.25^\circ \times 0.25^\circ$ (~27 km), and we applied the bilinear resampling techniques for downscaling to a fine resolution of 250 m [50]. Accordingly, the data were downloaded, resampled, and extracted to a spatial extent for encompassing the study region. Using the formula mentioned in Table 2, the PCI was calculated for October, November, and December for the five years of study period (2014–2018 CE). It was further downsampled to a spatial resolution of 30 m, so that all indices could maintain the same pixel size.

Temperature-condition index (TCI) is one of the essential indices used to understand the climatic signs and soil-moisture content in a region [51,52]. It detects the effect of thermal stress on vegetative growth and intensity of dryness. The thermal infrared sensor (TIRS) of Landsat 8 OLI was utilized to derive the TCI and the land-surface temperature (LST) was extracted from the thermal band of Landsat 8 using the split-window algorithm [53,54]. TCI was calculated from the minimum and maximum pixel values of LST. The minimum, maximum, and monthly LST were extracted for a time series (2014–2018 CE) to compute TCI using the equation mentioned in Table 2.

Vegetation-condition index (VCI) monitors drought-affected regions with the long-term normalized-difference vegetation index (NDVI) values [55,56]. The VCI and TCI are inversely proportional, as vegetation growth is affected by temperature intensity. In order to quantify vegetation stress, the NDVI is a useful tool, with the limitation that it detects only short-term variations in vegetation deficiency [57,58]. The VCI, however, detects long-term vegetation-drought severity [51]. Based on red and near-infrared (NIR) bands in Landsat 8, we calculated the NDVI for the study period (2014–2018 CE) and extracted VCI with the multiple time series of NDVI (equation mentioned in Table 2) with the minimum ($NDVI_{min}$) and maximum ($NDVI_{max}$) values.

Scaled drought-condition index (SDCI) is an advanced remote-sensing index for monitoring agricultural drought severity conditions [59]. It provides better results compared to other indices (i.e., NDVI, VCI, and VHI) for screening drought-affected areas. It is a multi-sensor drought index, computed by integrating precipitation deficiency as PCI, temperature variation as TCI, and vegetation stress as VCI, with the empirical weights of 0.5, 0.25, and 0.25, respectively [60,61]. The PCI was given higher empirical weightage as

it played a vital role in influencing the SDCI values [59]. We evaluated the agricultural drought after calculating SDCI, as described in Table 2.

3.3. Hydrological Drought

Standardized water-level index (SWI) scales the aquifer stress and fluctuation of groundwater table caused by hydrological droughts [62]. It is computed by dividing the standard deviation with the difference between the water level of the current month and the long-term mean value [5,13]. We selected around 75 wells for collecting the groundwater levels for evaluating the fluctuations. The monthly groundwater-level data from the PWD Chennai was used to compute the monthly SWI for the study period of 2014–2018 CE, and it was clipped to map the spatio-temporal distribution of hydrological drought using the equation mentioned in Table 2.

3.4. Multi-Drought Severity Index (MDSI)

Satellite-based drought assessment and monitoring are more effective as the data availability and the resolution (i.e., spatial and temporal) are high enough for regional/local-scale analysis. Drought complexity and its degree of severity are nevertheless evaluated with a single indicator, as they are the result of multiple influencing factors [6], and it is challenging to determine multiple severity factors in a single index. Several drought indices are still used (i.e., vegetation-drought-response index [63] and vegetation outlook [64]), and they require multiple satellite data and in situ weather and biophysical data. However, it is difficult to apply these indices to different spatial extents due to data constraints. The drought indices adopted for different climatic conditions are developed only by integrating (i.e., blending) multiple remote-sensing-based indices and factors. The blending of remote-sensing-index techniques was implemented by Heim [65] and several blended hybrid remote-sensing indices, which are helpful in drought monitoring, were developed (VCI [55], VHI [56], SDCI [59]) as a consequence. Accordingly, the multi-drought severity index (MDSI) is introduced to understand dynamic drought phenomena and multi-aspect influences on drought intensity in the study area. The seasonal mean value of meteorological (SPI), agricultural (SDCI), and hydrological droughts (SWI) was computed, and its empirical weightage was assigned through a linear combination approach [51,59]. The seasonal mean indices of SPI, SDCI, and SWI were blended through equation mentioned in Table 2 to compute the MDSI, which is a standardized scaled index used to portray regions affected by three types of drought (meteorological, agricultural, and hydrological). The blending process of remote-sensing indices includes assigning appropriate weights for multiple factors, which is a difficult process and requires a suitable technique, for which equal weighting and linear combination approaches are commonly used. Here, equal weights were applied to meteorological (0.3) and hydrological droughts (0.3), while the weightage of agricultural droughts (0.4) was slightly increased as the study region is exposed to such droughts frequently.

3.5. Socio-Economic Vulnerability (SEV)

Almost every natural calamity involves social and economic aspects. In the case of drought, there is an absolute crisis at the socio-economic level; this study assesses the socio-economic vulnerability of the study area. We considered four key factors, population density (PD), household density (HD), literacy ratio (LR), and working population ratio (WPR) [36–38,66], to compute the socio-economic vulnerability with the equation in Table 2. These were computed with the integration (i.e., sum) of PD, HD, LR, and WPR, and the vulnerability scale, ranges from 1 to 5, was classified into five classes such as very high, high, moderate, low and very low [67].

Table 2. The formula/index adopted for the study to compute the drought indices and socio-economic vulnerability.

Formula/Index	Description
$SPI = \frac{(X_{ij} - X_{im})}{\sigma}$	SPI is standardized precipitation index, X_{ij} is the precipitation of i th month and i th year, X_{im} is mean of the seasonal precipitation received by the same rain-gauge station, and σ is the standard deviation. It categorizes the severity of meteorological drought into seven major classes, extending from extremely dry to extremely wet (Table 3) [45].
$PCI = \frac{(TRMM - TRMM_{min})}{(TRMM_{max} - TRMM_{min})}$	PCI is precipitation-condition index, TRMM is a pixel value of monthly precipitation, and $TRMM_{max}$ and $TRMM_{min}$ are maximum and minimum values of the same months of the year between 2014 and 2018 CE. The intensity of drought severity based on the PCI value ranges from 0 to 1 (Table 4). The values nearest to 1 are characterized as no drought (wet condition), and values nearest to 0 represent extreme drought [2].
$TCI = \frac{(LST_{max} - LST_i)}{(LST_{max} - LST_{min})}$	TCI is temperature-condition index, LST_i is a pixel value of the current month temperature, LST_{max} and LST_{min} are the absolute maximum and minimum LST values in multiple years. The severity range of TCI values varies from 0 to 1 (Table 4). Values closer or equal to 0 denote dry conditions with abnormal temperatures, and values nearer to 1 represent wet conditions with adequate temperatures [51].
$VCI = \frac{(NDVI_i - NDVI_{min})}{(NDVI_{max} - NDVI_{min})}$	VCI is vegetation-condition index, $NDVI_i$ is pixel range of current month NDVI, and $NDVI_{min}$ and $NDVI_{max}$ are the minimum and maximum values of temporal NDVI. The vegetation stress is indicated with VCI varying from 0 to 1 (Table 4) indicating a range of intense vegetation stress to optimal vegetation conditions [55].
$SDCI = 0.25 \times TCI + 0.50 \times PCI + 0.25 \times VCI$	SDCI is scaled drought-condition index, with the agricultural drought severity varying between 0 and 1 (Table 4). The values nearest to 0 represent extreme drought, and the values nearest to 1 suggest no drought [59].
$SWI = \frac{(W_{ij} - W_{im})}{\sigma}$	SWI is standardized water-level index. W_{ij} is a water level of i th month and i th year, W_{im} is the seasonal mean of the same well, and σ is the standard deviation. The values of SWI varying between 0 and 2 suggest different degrees of hydrological drought (Table 5) [62].
$MDSI = 0.30 \times SPI + 0.40 \times SDCI + 0.30 \times SWI$	The MDSI is multi-drought severity index, and its severity values vary from 0 to 1, reflecting the potential effect of multi-drought. The values nearest to 0 represent extremely unfavorable drought conditions, and vice versa.
$PD = \frac{\text{Number of Population}}{\text{Total Geographical Area}}$	PD is population density. The total populations of the villages were divided by geographical area (km^2) of the village [63].
$HD = \frac{\text{Number of Households}}{\text{Total Geographical Area}}$	HD is household density. The total number of households in each village was divided by geographical area (km^2) of the village [36].
$LR = \frac{\text{Total Literate Population}}{\text{Total Population}}$	LR is literacy ratio. The total number of literate individuals was divided by total population in the villages [37].
$WPR = \frac{\text{Total Working Population}}{\text{Total Population}}$	WPR is working population ratio. The total number of working individuals was divided by total population in the villages.
$SEV = \sum(PD, HD, LR, WPR)$	SEV is socio-economic vulnerability. Summation of normalized PD, HD, LR, and WPR and its severity scale varies from 1 to 5 [67].

Table 3. Severity of meteorological drought classes (SPI) based on McKee et al. [45]’s classification.

Drought Classes	SPI Values
Extremely dry	<−2
Severely dry	−1.5 to −1.99
Moderately dry	−1.0 to −1.49
Near normal	−0.99 to 0.99
Moderately wet	1.0 to 1.49
Very wet	1.5 to 1.99
Extremely wet	>2.0

Table 4. Values of different agricultural drought classes are based on the PCI, TCI, VCI, and SDCI indices [2,51,55,59].

Drought Classes	Values	PCI	TCI	VCI	SDCI
Extreme Drought	<0.10				
High Drought	0.11–0.20				
Moderate Drought	0.21–0.30				
Slight Drought	0.31–0.40				
No Drought	>0.40				

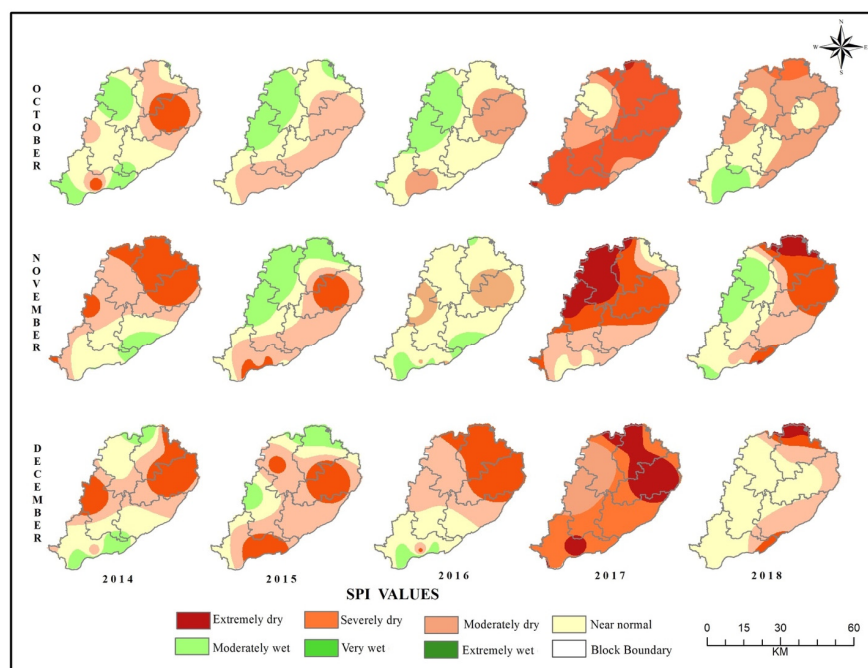
Table 5. Values of different hydrological drought classes (SWI) are based on Bhuiyan [62]’s classification.

Drought Classes	SWI Values
Extremely Drought	>2
High Drought	1.5 to 1.99
Moderate Drought	1.0 to 1.49
Slight Drought	0.99 to 0.00
No Drought	<0

4. Results

4.1. Meteorological Drought

The SPI values for the three months (October, November, and December) over the five years were used to examine the rainfall during the northeastern monsoon season (Figure 3, Table 3). These values demarcated the areas as extremely dry, severely dry, moderately dry, near normal, moderately wet, very wet, and extremely wet. We did not notice very wet or extremely wet areas in any of the years, and the meteorological drought generally ranged from moderately wet to extremely dry, except for 2017 CE. The study area remained moderately wet to moderately dry in October of 2015 CE and 2016 CE, and moderately dry to extremely dry in December of 2017 CE. We did not detect the extremely dry class in 2014 CE, 2015 CE, or 2016 CE. The extremely dry class was noted only in the years 2017 and 2018. The year 2017, it was noted to be the most vulnerable year, during which the extremely dry class was distributed intensely in the blocks of Sendurai and Ariyalur in the month of November and in the blocks of Andimadam and Jayamkondam in the month of December. Next, the severely dry class was observed in the northeast of the study area (i.e., Andimadam and Jayamkondam blocks) and the moderately dry class covered a large portion of the study area during the three months of 2017 CE. This shows that the rainfall was deficient in 2017 CE, as there were no wet classes in the SPI. The extremely dry and severely dry classes, however, had relatively less coverage in 2018 CE. The occurrence of the extremely dry class in the years 2017 CE and 2018 CE suggests insufficient precipitation, suggesting the risk of meteorological drought in the study area.

**Figure 3.** Spatio-temporal distributions of standardized precipitation index (SPI) and different degrees of drought in Ariyalur district of southern India.

4.2. Agricultural Drought

The precipitation-condition index (PCI) is an influencing factor in agricultural drought analysis as its values are directly proportional to the level of precipitation. It was used to categorize the regions of extreme, high, moderate, slight, and no drought (Figure 4a, Table 4). The outcome illustrates that extreme drought was present in all the years. Except for 2017 CE and December 2016 CE, the precipitation pattern of the study area was divided into five different classes, ranging from no drought to extreme drought. The precipitation in 2017 CE and December of 2016 CE did not show no-drought or slight-drought regions. The entire area was divided into moderate drought to extreme drought due to insufficient seasonal rainfall in 2017 CE.

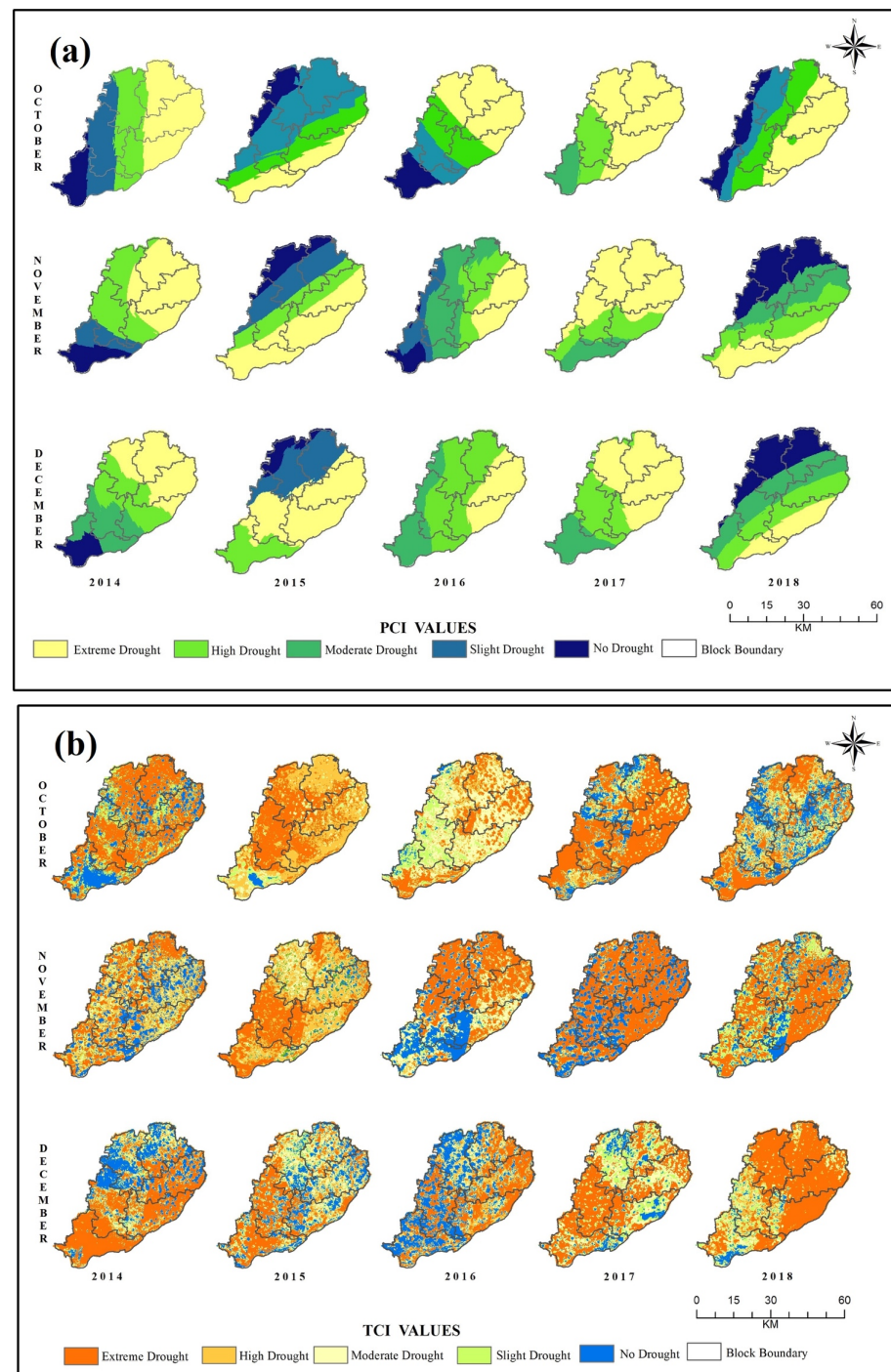


Figure 4. Cont.

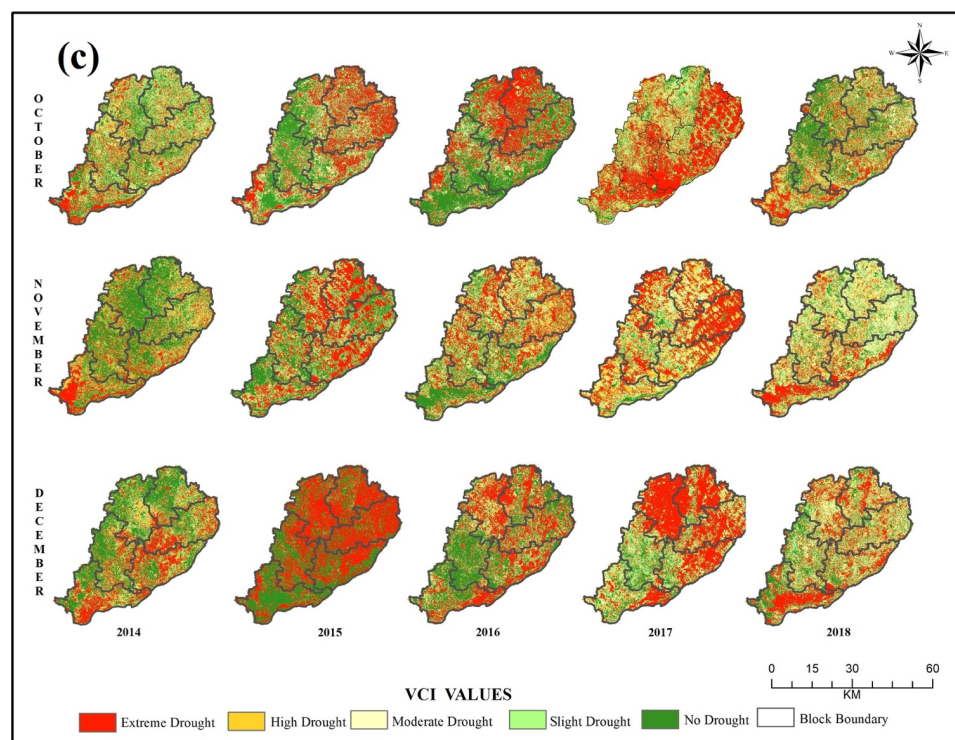


Figure 4. Spatio-temporal distributions of agricultural drought and different degrees of severity in Ariyalur district of southern India: (a) precipitation-condition index (PCI); (b) temperature-condition index (TCI); (c) vegetation-condition index (VCI).

The temperature-condition index (TCI) is a direct indicator of the heat that prevailed in the study area, and it was derived from the land-surface temperature for the years between 2014 and 2018 CE (Figure 4b, Table 4). The values, subdivided into five classes, classed the area as having extreme, high, moderate, slight, or no drought. The values exhibited extreme and high drought more frequently, and the areas of slight and no drought were in minor patches. The influence of the temperature on the level of drought was comparatively low in 2015 CE and 2016 CE. By contrast, the higher temperatures of 2014 CE, 2017 CE and 2018 CE led to extreme and high levels of drought. Similar to the PCI values, the TCI also recorded extreme drought conditions in several areas in 2017 CE.

The vegetation-condition index (VCI) is the graphical indicator of the vegetation stress, and it was derived from the quantitative values of NDVI. It indicated the prevailing vegetation condition in the study area for 2014–2018 CE (Figure 4c). The five classes demarcated the areas of extreme, high, moderate, slight, and no drought (Table 4). The no-drought classes were mostly observed in 2014 CE and 2015 CE, and the coverage of this area slightly decreased in 2016 CE. Eventually, the coverage of the extreme and high drought classes was higher in proportion in 2017 CE.

The spatial distribution of the scaled drought-condition index (SDCI) categorized the study area into five different classes (extreme, high, moderate, abnormally dry, and no drought), as shown in Figure 5 and Table 4. The spatio-temporal view resembles the pattern of the VCI. The extreme- and high-drought classes were scattered all over the study region in all the months of every year with an intensified pattern, but had only minor coverages in 2014 CE. Eventually, both of these classes increased moderately in the east and south of the study area (near the Jayankondam, T.Palur, and Thirumanur blocks) in 2015 CE and 2016 CE. The abundance of drought-stricken crops increased slightly. The extreme drought class had the highest coverage in 2017 CE and the areas with no drought remained the least common. The extreme drought of 2017 CE indirectly nullified the no-drought class for the region, especially during the month of November. Furthermore, in the year 2018, the extreme-drought-class region reduced in comparison with the previous years. The

SDCI monitoring suggests that the vegetation health in parts of Jayankondam, T.Palur, and Thirumanur blocks had suffered significant damage. The no-drought condition had the highest coverage in 2014 CE.

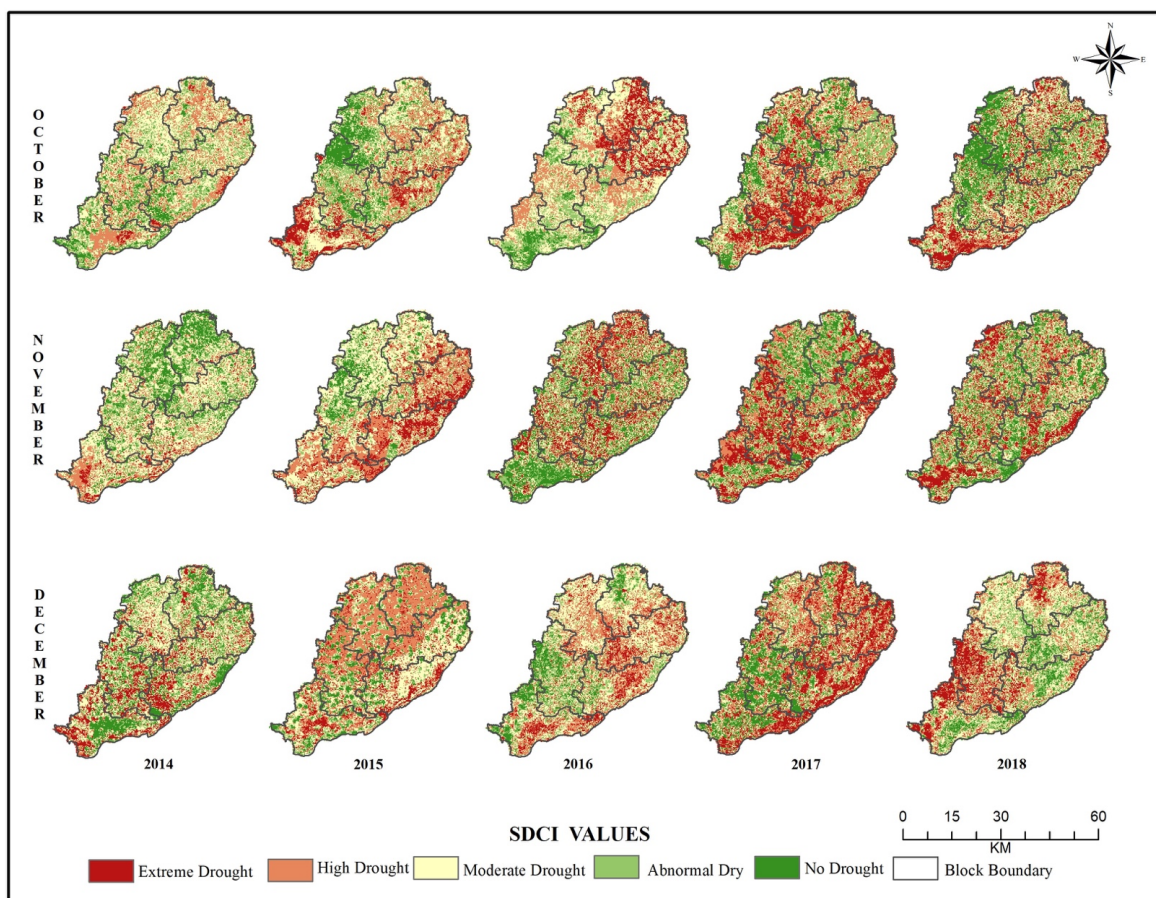


Figure 5. Spatio-temporal distributions of scaled drought-condition index (SDCI) and different degrees of drought in Ariyalur district of southern India.

4.3. Hydrological Drought

The standard water-level index (SWI) characterized the groundwater stress as its values precisely reflected the groundwater levels. The quantitative assessment of the SWI between 2014 and 2018 CE classified the areas as having extreme, high, moderate, slight, and no drought (Figure 6, Table 5). In 2014 CE, the proportion of slight-drought areas was high, and a minimal number of areas had a high level of drought. A significant part of the study area indicated no drought both in 2014 CE and in 2015 CE, as this region received more rainfall, as shown on the SPI map (Figure 3). The no-drought areas in 2015 CE covered the western and southern parts of the study area (i.e., Ariyalur, Sendurai, and Thirumanur blocks, Figure 1), whereas the northern, northeastern, and southwestern areas covering Andimadam, Jayamkondam, and T. Palur mostly featured the moderate- and high-drought SWI class. The areas of slight and no drought were modified into moderate- and high-drought conditions in 2016 CE. Eventually, the coverages of the extreme and high drought conditions peaked in 2017 CE, mirroring the PCI and SPI values. This extreme drought class was mostly concentrated over the Sendurai, Andimadam, and Jayamkondam blocks. However, these drought-class areas changed to high and moderate drought in 2018 CE, and some areas in the northern and southern tip became no-drought areas.

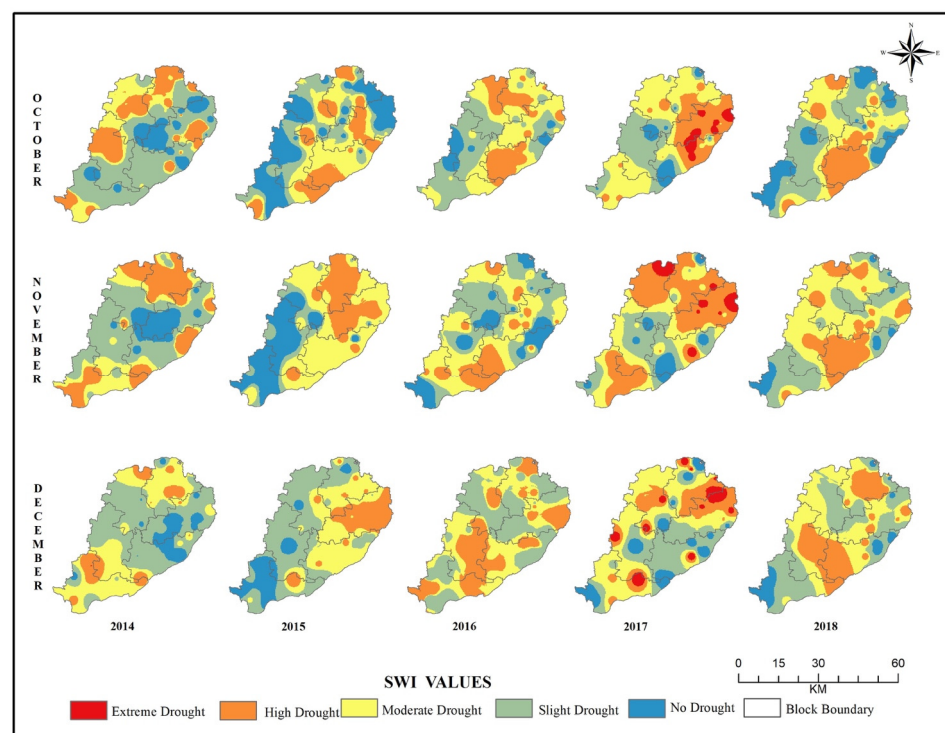


Figure 6. Spatio-temporal distributions of standard water-level index (SWI) and different degrees of drought in Ariyalur district of southern India.

4.4. Socio-Economic Vulnerability (SEV)

We derived the socio-economic vulnerability from the parameters of the population density, household density, literacy ratio, and working-population ratio. This separated the study area into very high, high, moderate, low, and very low classes following the rankings of the influencing parameters. The population density and household density showed similar patterns, as these parameters are interlinked (Figure 7a,b). The areas with high classes were mostly in the northeastern blocks (Andimadam and Jayamkondam). In these blocks, the population and household density are higher than in the other blocks of Sendhurai and Ariyalur, where most of the region falls under the moderate-density class of both population and household. It was then inferred that the literacy ratio was inferior as one-third of the region remained in the very-high-vulnerability class, mostly in the middle and southeastern parts covering most of Ariyalur, T.Palur, and a minor portion of Thirumanur block (Figure 7c). The very-high-vulnerability literacy class was also noticed over the northernmost area of the Sendhurai block, in the Ariyalur district. The working-population ratio showed a very-high-vulnerability class in Sendhurai and Jayamkondam, whereas the highly vulnerable class was mostly concentrated over the Jayamkondam block in the study region (Figure 7d). The final map of the socio-economic vulnerability demarcated the areas of the very-high and high classes, which mostly resembled the distributions of the population density and household density (Figure 7e). The Thirumanur block in south of the study area had low socio-economic vulnerability as the block features a population that is of mostly low vulnerability and household density. The Andimadam and Jayamkondam blocks, in the northeast of the study area, exhibited the worst socio-economic conditions; their populations belonged to the highly vulnerable class of socio-economic vulnerability, as these blocks mostly include the highly vulnerable class of the population, a high level of household density, and a high working-population ratio. Hence, these blocks were identified as possessing very high socio-economic vulnerability, with less of an ability to overcome severe droughts.

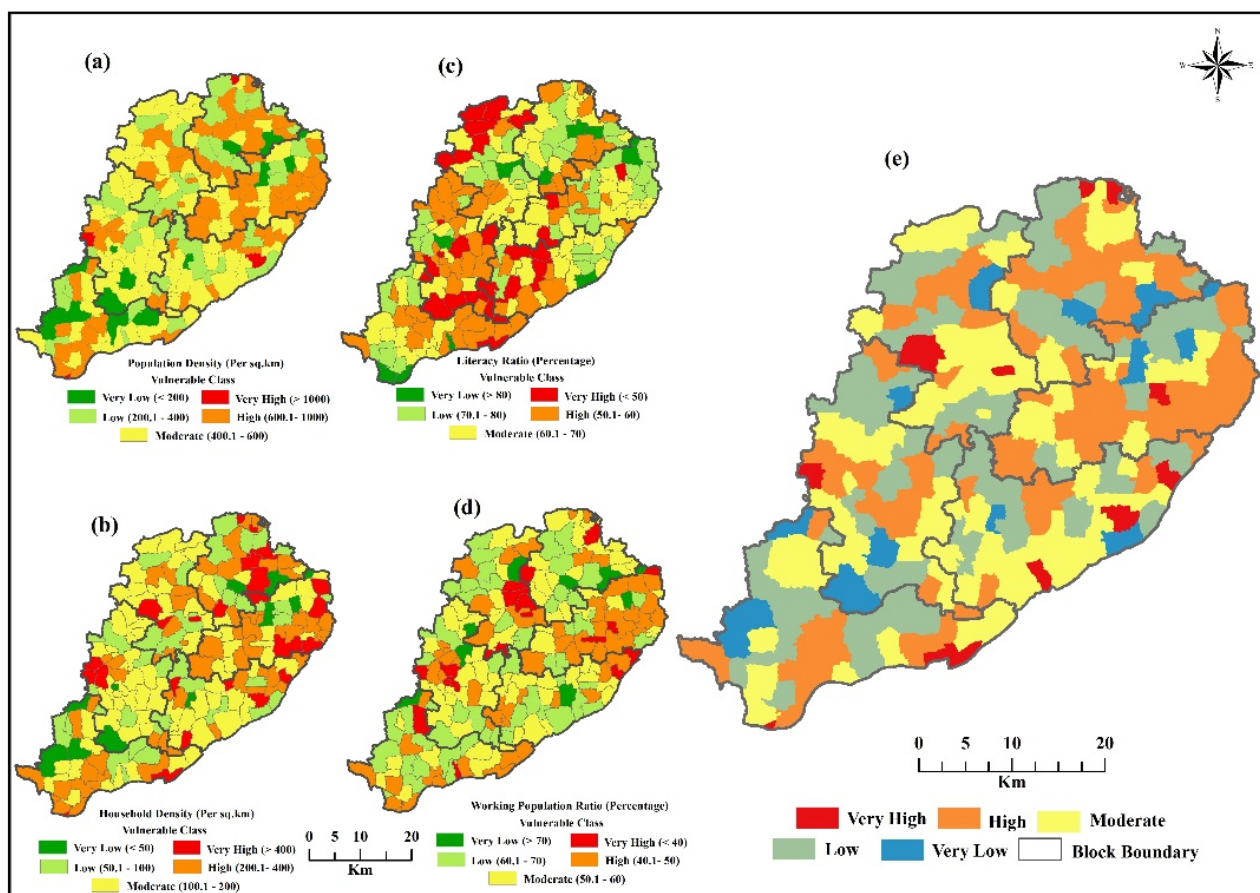


Figure 7. Spatial distributions of: (a) population density (PD), (b) household density (HD), (c) literacy ratio (LR), (d) working-population ratio (WPR), and (e) socio-economic vulnerability (SEV) in Ariyalur district of southern India.

4.5. Multi-Drought Severity Index (MDSI)

The analysis and monitoring of the multi-aspect drought severity in this study for the eastern part of Tamil Nadu, Ariyalur district, were carried out with several indices through the evaluation of the combined effects of meteorological (SPI), agricultural (SDCI), and hydrological (SWI) droughts on a scaled value, i.e., the multi-drought severity index (MDSI), by applying the empirical weights to the SPI, SDCI, and SWI (Figure 8a–c). Thus, the results of the MDSI presented a similar distribution of results to those observed in the three indices (i.e., SPI, SDCI, SWI), in accordance with the weights assigned to it. The Jayankondam block and a small portion of the Tirumanur block were adversely affected by all three drought types (Figure 8a–c), which implies the same as the MDSI results. Furthermore, the Ariyalur block of the study area experienced no drought for SPI, SDCI, and SWI, which perfectly matched the MDSI result. Thus, the results of the MDSI strongly reflected the weights assigned. The spatial variation in the MDSI, scaled in five classes of severity condition (very high, high, moderate, low, and very low), is presented in Figure 8d. The western part (i.e., Ariyalur and Sendurai blocks) was less affected, with a low-to-very-low severity class. On the other hand, the eastern part (i.e., Jayankondam and T.Palur blocks) was enormously affected, with the severity class ranging from moderate to very high. The very-high class was mainly concentrated in the Jayankondam block, as well as in some minor parts of the T.Palur and Thirumanur blocks. The major parts of both the latter blocks exhibited moderate- and high-severity droughts.

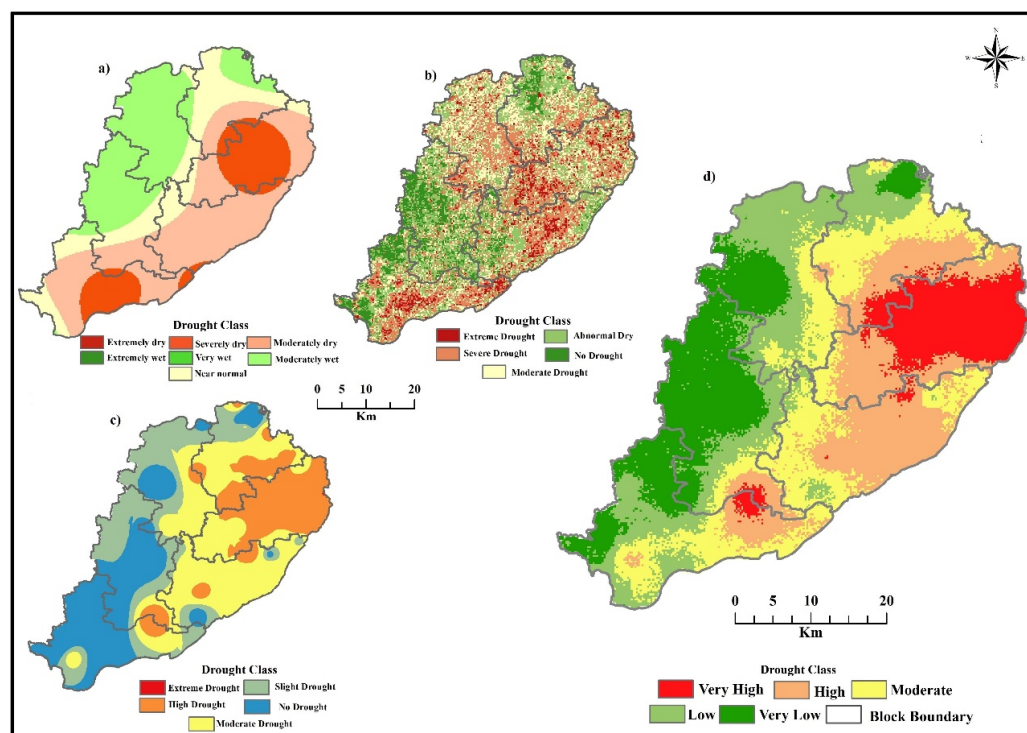


Figure 8. Seasonal mean of: (a) meteorological drought, (b) agricultural drought, (c) hydrological drought, and (d) multi-drought severity index (MDSI) in Ariyalur district of southern India.

5. Discussion

The quantitative temporal analysis of the meteorological, hydrological, and agricultural droughts during 2014–2028 CE revealed extreme and severe droughts in 2017 CE. This suggests that if the frequency and probability persist, the study region will experience severe meteorological droughts, as in 2017 CE (Figure 3), more frequently in the near future. Murthy et al. [68] and Guhathakurta et al. [69] suggest a high probability of drought in Tamil Nadu, in south India, and Dhiman [70] states that most of the districts in Tamil Nadu are overexploiting groundwater due to monsoonal failure. Similarly, Chandrasekar et al. [71], Varadan and Kumar [72], Vaani and Porchelvan [73], Balasundareswaran et al. [74], and Das et al. [75] suggested that the Ariyalur district is the most vulnerable, with moderate-to-high agricultural drought.

Thus, the combined effect of insufficient rainfall and overexploited groundwater in the eastern blocks (Jayankondan and T. Palur) led to crop failure, suggesting severe agricultural droughts. This crop failure directly constitutes the effect on the paddy, which is the major crop found in the Ariyalur district and in a significant portion of T. Palur and Jayankondan blocks. If these conditions of severe drought persist over a longer period, they may have a substantial impact on the paddy crop, and the crop pattern will be probably change to that of the groundnut crop that is present over the T. Palur block. This will affect the production of paddy and increase the demand for food crops. Thus, the persistence of this severe drought condition for a prolonged period of time over the region will trigger famine. In the present study, it is concluded from the MDSI (Figure 8d) that the entire eastern region is already facing the worst conditions. If the vulnerable situation, probability, and frequency pattern persist over a longer period of time, the drought affecting these areas could extend to the western region in the future.

The Jayankondam block was the most affected area with the combined influences of meteorological, agricultural, and hydrological droughts, highlighting its extreme vulnerability. The very high agricultural droughts (SDCI) of 2015 CE and 2016 CE were mainly due to low precipitation (PCI, Figure 4a) and high temperatures (TCI, Figure 4b). For the meteorological drought (SPI), the Jayankondam rain-gauge stations recorded lower

amounts of rainfall during the northeast monsoon season, except in October and November of 2016 CE (Figure 3). The hydrological drought analysis (SWI) also suggested high aquifer stress and extreme drought, particularly in 2015, 2017, and 2018 CE (Figure 6). The MDSI characterized this area as an extreme-drought-affected block. This cumulative-stress drought condition implies a life-threatening impact on the food crops, leading to famine in the eastern part of the study area. The most severely affected crops in this block include paddy, maize, and cotton (Figure 1b). The distribution of paddy is the most significant of these, and it will be profoundly affected by insufficient rainfall and aquifer stress aquifers. Crop growth would imply a lower level of groundwater. The drought severity by block, in decreasing order, is as follows: T.Palur block in the east, Andimadam block in the north, and Thirumanur block in the south of the study area (Figure 8d). In terms of the SDCI, these blocks were severely affected between 2015 and 2017 CE, with low TCI and PCI values. These regions were also affected by highly fluctuating groundwater levels due to over-exploitation for domestic purposes and the irrigation of crops, which potentially lead to aquifer stress (SWI). The SPI values classified these areas as suffering from moderate-to-very-high drought because of the reduced seasonal rainfall in the years 2015, 2017, and 2018 CE (Figure 3). The cultivations of paddy, sugarcane, groundnut, and maize were sparse due to the scarcity of water.

The fulfilment of the framework was achieved as the results of this study were compared with the socio-economic variable, which is strongly associated with the power of individuals to withstand drought conditions. Vengateswari et al. [76] infer that the southern part of India (Tamil Nadu) is exposed to a moderate-to-high frequency of meteorological droughts and that droughts occurred in the Ariyalur district approximately 8 times over 37 years of the northeastern monsoon season, and Balaganesh et al. [77] state that the Ariyalur district has drought vulnerability with high sensitivity and low adaptive capacity. Moreover, the results of the MDSI, with respect to socio-economic vulnerability, suggest that the Jayankondam block in the east was extremely affected, and that it has less of an ability to overcome severe droughts. This condition is mainly due to its higher population and household density, leading to higher potential resource utilization, which reduces the possibility of recovery under the existing environmental conditions. The blocks in the north, south, and east (i.e., T.Palur, Thirumanur, and Andimadam) are in an endangered position, as both their MDSI and their socio-economic vulnerability are in the medium-to-high vulnerability categories. This is mainly due to the significant increase in the household density across these blocks, which implies an increasing demand for food crops, such as, paddy, which in turn requires a substantial supply of water, which is limited in the T.Palur, Thirumanur, and Andimadam blocks due to meteorological and hydrological drought. These blocks require initial retrieval practices to recover. Thus, to improve the livelihoods of households, the crop paddy can be replaced with a drought-resistant crop, groundnut, which requires a minimum amount of water consumption in comparison with the paddy.

Hence, the outcomes of this study and the field-visit photography (Figure 9) demonstrate that Jayankondam block is a highly drought-prone region, while T. Palur and Andimadam blocks are moderately drought-prone. This is mainly due to the absence of a surface-water system, which makes Jayankondam highly sensitive and less adaptive. The T. Palur and Andimadam blocks benefit from the water resources of the Vellar and Kollidam rivers, contributing to their potential recovery. Additionally, the use of groundwater is restricted in the three blocks due to higher levels of physio-chemical contamination [78]. All these factors combine to create dramatically unfavorable conditions for the individuals in the study area. Thus, management strategies have to be adopted immediately in the Jayankondam block to ensure rapid recovery. Furthermore, structural and non-structural measures should be implemented for long-term operations. The full recommendations for the drought-severity blocks highlighted in the study are as follows:

1. The results exemplify that the socio-economic conditions of the Jayankondan block must be strengthened to manage the existing conditions, as the occurrence of meteorological and hydrological droughts will be more frequent in the near future, due to global warming.
2. The high-priority region (i.e., Jayankondan block) requires closer agricultural drought monitoring through the implementation of a real-time early-warning system, through which prediction models can be developed to mitigate the prevalence of drought.
3. A multi-cropping pattern and a drought-resistant crop must be used to maintain the sustainability of soil nutrients.
4. The region features weak socio-economic conditions, which must be strengthened by increasing the literacy rate and conducting awareness programs for agricultural workers.
5. A proper irrigation system should be maintained for seasonal crops, and as a water conservation plan; rainwater harvesting must be implemented to replenish ground-water levels.
6. Policymakers should consider investment in agro-based projects (i.e., small-scale water conservation and management) at the micro-level, subsidies for agricultural activities, crop insurance plans, emergency disaster funds, and immediate remedial action during monsoon failure).

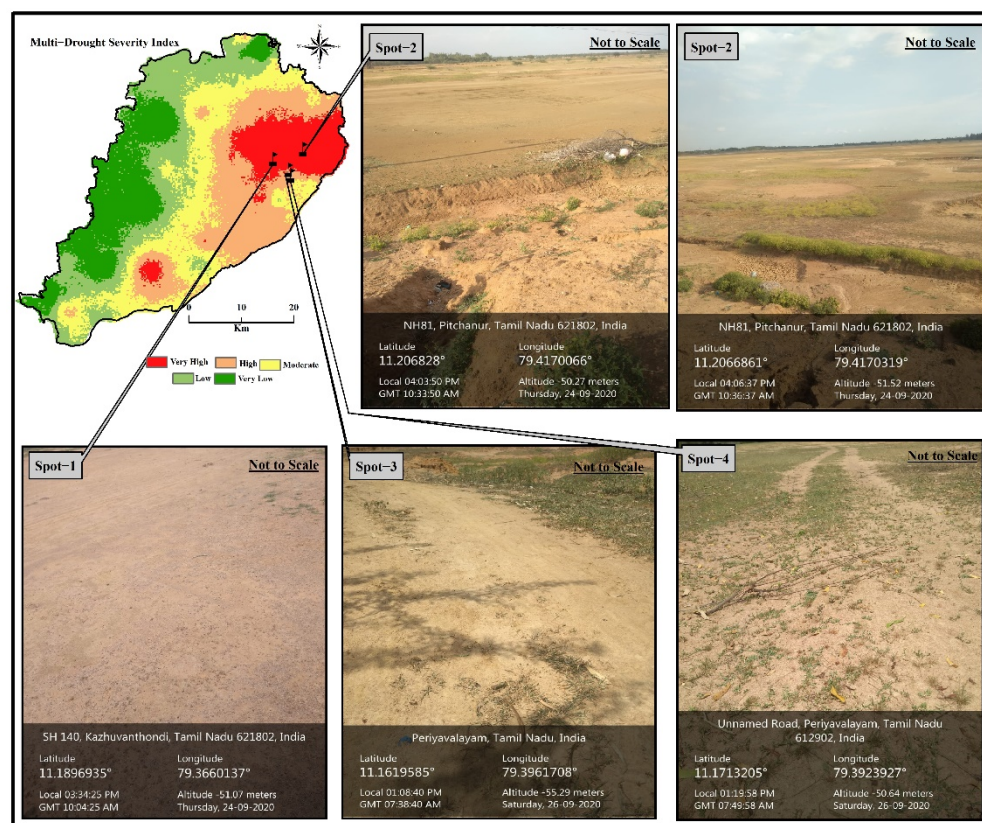


Figure 9. Multi-drought severity (i.e., meteorological, agricultural, hydrological), and field photographs of extreme-drought region (i.e., Jayankondam block), which implies that the region is exposed to extreme drought conditions.

6. Conclusions

A framework was adopted to analyze the MDSI and identify vulnerable areas by comparing the socioeconomic conditions through regions' drought tolerance and sensitivity, as well as the resilience of individuals to the consequences of drought in Tamil Nadu, India. This study's major findings suggest that the combined influences of inadequate rainfall and the over-exploitation of groundwater have caused agricultural stress in Jayankondan, T.Palur, and Andimadam blocks. When comparing these result with the socioeconomic

condition, it was found that Jayankondan, in the eastern part of the study area, is highly affected, as the higher population and household density force the overexploitation of the resources present in the study region. On the other hand, T.Palur and Andimadam blocks fall under moderate socioeconomic stress as they benefit from the availability of surface water through the Kollidam and Vellar rivers. Therefore, long-term drought-management measures should be followed in the area exposed to extreme drought severity (i.e., Jayankondan), and short-term practices should be implemented in the moderate-severity areas (i.e., T.Palur and Andimadam). As the socioeconomic conditions are also declining in these blocks, however, special attention must be given to drought preparedness to strengthen the blocks' adaptive capacity. The construction of surface canals along drought-affected regions to manage the short-term effects of drought, and crop rotation must be practiced in drought-affected agricultural areas to maintain soil-moisture and nutrient levels. The results reported in this study certainly help to improve existing or generate new strategies to minimize the drought conditions in the case-study area.

Author Contributions: V.R., K.K., T.P. and J.K.: conceptualization, methodology, formal analysis, project administration, visualization, field visit, writing—original draft. P.D.R. and L.C.: supervision, validation, writing—review and editing. S.S. and M.P.: methodology, writing—original draft. All authors have read and agreed to the published version of the manuscript.

Funding: This research received no external funding.

Institutional Review Board Statement: Not applicable.

Informed Consent Statement: Not applicable.

Data Availability Statement: The datasets used during the current study are available from the USGS GloVis portal (<https://glovis.usgs.gov/app>, accessed on 12 July 2019), TRMM (<https://gpm.nasa.gov/data-access/downloads/trmm>, accessed on 16 July 2019) and Census data (<https://censusindia.gov.in/>, accessed on 31 July 2019). The datasets generated and analyzed during the current study are available from the corresponding author on reasonable request.

Acknowledgments: The authors would like to acknowledge the Department of Geography and the Department of Remote Sensing, Bharathidasan University, Tiruchirappalli, for their coordinative involvement and support in utilizing the laboratory facilities, and also thank the faculty members of the respective departments.

Conflicts of Interest: The authors declare no conflict of interest.

References

1. Jasem, A.H.; Alraggad, M. Assessing Groundwater Vulnerability in Azraq Basin Area by a Modified DRASTIC Index. *J. Water Resour. Prot.* **2010**, *2*, 944–951. [CrossRef]
2. Tian, Q.; Yu, T.; Du, L.; Tian, Q.; Yu, T.; Meng, Q.; Jancso, T.; Udvardy, P.; Huang, Y. A comprehensive drought monitoring method integrating MODIS and TRMM data. *Int. J. Appl. Earth Obs. Geoinf.* **2013**, *23*, 245–253. [CrossRef]
3. Mohammad, A.H.; Almomani, T.; Alhejoj, I. Groundwater Vulnerability for the Surface Outcropping Aquifers in Jordan. *J. Environ. Prot.* **2015**, *6*, 250–258. [CrossRef]
4. Hussein, H. The Guarani Aquifer System, highly present but not high profile: A hydropolitical analysis of transboundary groundwater governance. *Environ. Sci. Policy* **2018**, *83*, 54–62. [CrossRef]
5. Mohammad, A.H.; Jung, H.C.; Odeh, T.; Bhuiyan, C.; Hussein, H. Understanding the impact of droughts in the Yarmouk Basin, Jordan: Monitoring droughts through meteorological and hydrological drought indices. *Arab. J. Geosci.* **2018**, *11*, 103. [CrossRef]
6. Park, S.; Im, J.; Jang, E.; Rhee, J. Drought assessment and monitoring through blending of multi-sensor indices using machine learning approaches for different climate regions. *Agric. For. Meteorol.* **2016**, *216*, 157–169. [CrossRef]
7. Trenberth, K.E.; Dai, A.; Rasmussen, R.M.; Parsons, D.B. The changing character of precipitation. *Bull. Am. Meteorol. Soc.* **2018**, *84*, 1205–1217. [CrossRef]
8. Trenberth, K.E.; Overpeck, J.T.; Solomos, S. Exploring Drought and Its Implications for the Future. *Eos Trans. Am. Geophys. Union* **2004**, *85*, 26. [CrossRef]
9. Wetherald, R.T.; Manabe, S. Detectability of summer dryness caused by greenhouse warming. *Clim. Change* **1999**, *43*, 495–511. [CrossRef]
10. Donald, W.A. Drought as a Natural Hazard: Concepts and Definitions Donald. In *Drought: A Global Assessment*; Donald, W.A., Ed.; Routledge: London, UK, 2000; pp. 3–18.

11. Rhee, J.; Im, J.; Park, S. Regional drought monitoring based on multisensor remote sensing. In *Remote Sensing of Water Resources, Disasters, and Urban Studies*; Thenkabail, P.S., Ed.; CRC Press: Boca Raton, FL, USA, 2015; pp. 401–415.
12. Dracup, J.A.; Lee, K.S.; Paulson, E.G. On the statistical characteristics of drought events. *Water Resour. Res.* **1980**, *16*, 289–300. [\[CrossRef\]](#)
13. Bhuiyan, C.; Singh, R.P.; Kogan, F.N. Monitoring drought dynamics in the Aravalli region (India) using different indices based on ground and remote sensing data. *Int. J. Appl. Earth Obs. Geoinf.* **2006**, *8*, 289–302. [\[CrossRef\]](#)
14. Wilhite, D.A.; Svoboda, M.D.; Hayes, M.J. Understanding the complex impacts of drought: A key to enhancing drought mitigation and preparedness. *Water Resour. Manag.* **2007**, *21*, 763–774. [\[CrossRef\]](#)
15. Kundu, A.; Dwivedi, S.; Dutta, D. Monitoring the vegetation health over India during contrasting monsoon years using satellite remote sensing indices. *Arab. J. Geosci.* **2016**, *9*, 144. [\[CrossRef\]](#)
16. Yu, C.; Li, C.; Xin, Q.; Chen, H.; Zhang, J.; Zhang, F.; Li, X.; Clinton, N.; Huang, X.; Yue, Y.; et al. Dynamic assessment of the impact of drought on agricultural yield and scale-dependent return periods over large geographic regions. *Environ. Model. Softw.* **2014**, *62*, 454–464. [\[CrossRef\]](#)
17. Wilhite, D.A.; Sivakumar, M.V.K.; Wood, D.A. Early Warning Systems for Drought Preparedness and Drought Management. In *Proceedings of the Expert Group Meeting, Lisbon, Portugal, 5–7 September 2000*; World Meteorological Organization: Lisbon, Portugal, 2000; pp. 161–176.
18. Mallya, G.; Mishra, V.; Niyogi, D.; Tripathi, S.; Govindaraju, R. Trends and variability of droughts over the Indian monsoon region. *Weather Clim. Extrem.* **2016**, *12*, 43–68. [\[CrossRef\]](#)
19. Bajgain, R.; Xiao, X.; Basara, J.; Wagle, P.; Zhou, Y.; Zhang, Y.; Mahan, H. Assessing agricultural drought in summer over Oklahoma Mesonet sites using the water-related vegetation index from MODIS. *Int. J. Biometeorol.* **2017**, *61*, 377–390. [\[CrossRef\]](#)
20. Zhang, T.; Simelton, E.; Huang, Y.; Shi, Y. A Bayesian assessment of the current irrigation water supplies capacity under projected droughts for the 2030s in China. *Agric. For. Meteorol.* **2013**, *178*–179, 56–65. [\[CrossRef\]](#)
21. Gao, Z.; Wang, Q.; Cao, X.; Gao, W. The responses of vegetation water content (EWT) and assessment of drought monitoring along a coastal region using remote sensing. *GIScience Remote Sens.* **2014**, *51*, 1–16. [\[CrossRef\]](#)
22. Dutta, D.; Kundu, A.; Patel, N.R.; Saha, S.K.; Siddiqui, A.R. Assessment of agricultural drought in Rajasthan (India) using remote sensing derived Vegetation Condition Index (VCI) and Standardized Precipitation Index (SPI). *Egypt J. Remote Sens. Sp. Sci.* **2015**, *18*, 53–63. [\[CrossRef\]](#)
23. Ghaleb, F.; Mario, M.; Sandra, A.N. Regional Landsat-Based Drought Monitoring from 1982 to 2014. *Climate* **2015**, *3*, 563–577. [\[CrossRef\]](#)
24. Sierra-Soler, A.; Adamowski, J.; Malard, J.; Qi, Z.; Saadat, H.; Pingale, S. Assessing agricultural drought at a regional scale using LULC classification, SPI, and vegetation indices: Case study in a rainfed agro-ecosystem in Central Mexico. *Geomat. Nat Hazards Risk* **2016**, *7*, 1460–1488. [\[CrossRef\]](#)
25. Khosravi, H.; Haydari, E.; Shekoohizadegan, S.; Zareie, S. Assessment the Effect of Drought on Vegetation in Desert Area using Landsat Data. *Egypt J. Remote Sens. Sp. Sci.* **2017**, *20*, S3–S12. [\[CrossRef\]](#)
26. Naumann, G.; Dutra, E.; Barbosa, P.; Pappenberger, F.; Wetterhall, F.; Vogt, J.V. Comparison of drought indicators derived from multiple data sets over Africa. *Hydrol. Earth Syst. Sci.* **2014**, *18*, 1625–1640. [\[CrossRef\]](#)
27. Santos, C.A.G.; Brasil Neto, R.M.; Passos, J.S.A.; da Silva, R.M. Drought assessment using a TRMM-derived standardized precipitation index for the upper São Francisco River basin, Brazil. *Env. Monit. Assess* **2017**, *189*, 250. [\[CrossRef\]](#)
28. Jiang, S.; Ren, L.; Zhou, M.; Yong, B.; Zhang, Y.; Ma, M. Drought monitoring and reliability evaluation of the latest TMPA precipitation data in the Weihe River Basin, Northwest China. *J. Arid. Land* **2017**, *9*, 256–269. [\[CrossRef\]](#)
29. Winkler, K.; Gessner, U.; Hochschild, V. Identifying droughts affecting agriculture in Africa based on remote sensing time series between 2000–2016: Rainfall anomalies and vegetation condition in the context of ENSO. *Remote Sens.* **2017**, *9*, 831. [\[CrossRef\]](#)
30. Livada, I.; Assimakopoulos, V.D. Spatial and temporal analysis of drought in Greece using the Standardized Precipitation Index (SPI). *Theor. Appl. Climatol.* **2007**, *89*, 143–153. [\[CrossRef\]](#)
31. Cancelliere, A.; Di Mauro, G.; Bonaccorso, B.; Rossi, G. Drought forecasting using the standardized precipitation index. *Water Resour. Manag.* **2007**, *21*, 801–819. [\[CrossRef\]](#)
32. Muthumanickam, D.; Kannan, P.; Kumaraperumal, R.; Natarajan, S.; Sivasamy, R.; Poongodi, C. Drought assessment and monitoring through remote sensing and GIS in western tracts of Tamil Nadu, India. *Int. J. Remote Sens.* **2011**, *32*, 5157–5176. [\[CrossRef\]](#)
33. Cruz-Roa, A.F.; Olaya-Marín, E.J.; Barrios, M.I. Ground and satellite based assessment of meteorological droughts: The Coello river basin case study. *Int. J. Appl. Earth Obs. Geoinf.* **2017**, *62*, 114–121. [\[CrossRef\]](#)
34. Bhavani, P.; Chakravarthi, V.; Roy, P.S.; Joshi, P.K.; Chandrasekar, K. Long-term agricultural performance and climate variability for drought assessment: A regional study from Telangana and Andhra Pradesh states, India. *Geomat. Nat Hazards Risk* **2017**, *8*, 822–840. [\[CrossRef\]](#)
35. Lik, B.; Rodell, M. Evaluation of a model-based groundwater drought indicator in the conterminous U.S. *J. Hydrol.* **2015**, *526*, 78–88. [\[CrossRef\]](#)
36. Aubrecht, C.; Ozceylan, D.; Steinnocher, K.; Freire, S. Multi-level geospatial modeling of human exposure patterns and vulnerability indicators. *Nat. Hazards* **2013**, *68*, 147–163. [\[CrossRef\]](#)

37. Ahsan, M.N.; Warner, J. The socioeconomic vulnerability index: A pragmatic approach for assessing climate change led risks-A case study in the south-western coastal Bangladesh. *Int. J. Disaster. Risk Reduct.* **2014**, *8*, 32–49. [\[CrossRef\]](#)
38. BalaSundareshwaran, A.; Abdul Rahaman, S.; Balasubramani, K.; Kumaraswamy, K.; Ramkumar, M. Habitat Risk Assessment Along Coastal Tamil Nadu, India—An Integrated Methodology for Mitigating Coastal Hazards. In *Coastal Zone Management*; Ramkumar, M., James, R.A., Menier, D., Kumaraswamy, K., Eds.; Elsevier: Burlington, NJ, USA, 2018. [\[CrossRef\]](#)
39. Törnros, T.; Menzel, L. Addressing drought conditions under current and future climates in the Jordan River region. *Hydrol. Earth Syst. Sci.* **2014**, *18*, 305–318. [\[CrossRef\]](#)
40. Patel, N.R.; Yadav, K. Monitoring spatio-temporal pattern of drought stress using integrated drought index over Bundelkhand region, India. *Nat. Hazards* **2015**, *77*, 663–677. [\[CrossRef\]](#)
41. Yaduvanshi, A.; Srivastava, P.K.; Pandey, A.C. Integrating TRMM and MODIS satellite with socio-economic vulnerability for monitoring drought risk over a tropical region of India. *Phys. Chem. Earth* **2015**, *83–84*, 14–27. [\[CrossRef\]](#)
42. Kamali, B.; Kouchi, D.H.; Yang, H.; Abbaspour, K. Multilevel drought hazard assessment under climate change scenarios in semi-arid regions-a case study of the karkheh river basin in Iran. *Water* **2017**, *9*, 241. [\[CrossRef\]](#)
43. Park, S.; Seo, E.; Kang, D.; Im, J.; Lee, M.-I. Prediction of drought on pentad scale using remote sensing data and MJO index through random forest over East Asia. *Remote Sens.* **2018**, *10*, 1811. [\[CrossRef\]](#)
44. Gnanachandrasamy, G.; Zhou, Y.; Bagyaraj, M.; Venkatramanan, S.; Ramkumar, T.; Wang, S. Remote Sensing and GIS Based Groundwater Potential Zone Mapping in Ariyalur District, Tamil Nadu. *J. Geol. Soc.* **2018**, *92*, 484–490. [\[CrossRef\]](#)
45. McKee, T.B.; Doesken, N.J.; Kleist, J. The relationship of drought frequency and duration to time scales. *Eighth Conf. Appl. Climatol.* **1993**, *17*, 179–183.
46. McKee, T.B.; Doesken, N.J.; Kleist, J. Drought monitoring with multiple time scales. In Proceedings of the 9th Conference on Applied Climatology, Dallas, TX, USA, 15–20 January 1995; pp. 233–236.
47. Oliver, J.E. Monthly Precipitation Distribution: A Comparative Index. *Prof. Geogr.* **1980**, *32*, 300–309. [\[CrossRef\]](#)
48. Yu, H.; Li, L.; Liu, Y.; Li, J. Construction of Comprehensive Drought Monitoring Model in Jing-Jin-Ji Region Based on Multisource Remote Sensing Data. *Water* **2019**, *11*, 1077. [\[CrossRef\]](#)
49. Sur, C.; Park, S.; Kim, T.; Lee, J. Remote Sensing-based Agricultural Drought Monitoring using Hydrometeorological Variables. *KSCE J. Civ. Eng.* **2019**, *23*, 5244–5256. [\[CrossRef\]](#)
50. Zeng, H.; Li, L.; Li, J. The evaluation of TRMM Multisatellite Precipitation Analysis (TMPA) in drought monitoring in the Lancang River Basin. *J. Geogr. Sci.* **2012**, *22*, 273–282. [\[CrossRef\]](#)
51. Kogan, F.N. Application of vegetation index and brightness temperature for drought detection. *Adv. Sp. Res.* **1995**, *15*, 91–100. [\[CrossRef\]](#)
52. Unganai, L.S.; Kogan, F.N. Drought Monitoring and Corn Yield Estimation in Southern Africa from AVHRR Data. *Remote Sens. Environ.* **1998**, *4257*, 219–232. [\[CrossRef\]](#)
53. Rongali, G.; Keshari, A.K.; Gosain, A.K.; Khosa, R. Split-Window Algorithm for Retrieval of Land Surface Temperature Using Landsat 8 Thermal Infrared Data. *J. Geovisualizat. Spat. Anal.* **2018**, *2*, 14. [\[CrossRef\]](#)
54. Venkatesh, R.; Abdul Rahaman, S.; Jegankumar, R.; Masilamani, P. Eco-Environmental Vulnerability Zonation in Essence of Environmental Monitoring and Management. *ISPRS Int. Arch. Photogramm. Remote Sens. Spat. Inf. Sci* **2020**, *XLIII-B5-2*, 149–155. [\[CrossRef\]](#)
55. Liu, W.T.; Kogan, F.N. Monitoring regional drought using the Vegetation Condition Index. *Int. J. Remote Sens.* **1996**, *17*, 2761–2782. [\[CrossRef\]](#)
56. Kogan, F.; Gitelson, A.; Zakarin, E.; Spivak, L.; Lebed, L. AVHRR-Based Spectral Vegetation Index for Quantitative Assessment of Vegetation State and Productivity: Calibration and Validation. In *Photogrammetric Engineering & Remote Sensing*; American Society for Photogrammetry and Remote Sensing: Baton Rouge, LA, USA, 2003; pp. 899–906.
57. Rouse, J.W.; Haas, R.; Schell, J.; Deering, D. Monitoring vegetation systems in the great plains with ERTS. In Proceedings of the Third Earth Resources Technology Satellite-1 Symposium, Washington, DC, USA, 10–14 December 1973; pp. 309–317.
58. Abdul Rahaman, S.; Venkatesh, R. Application of Remote Sensing and Google Earth Engine for Monitoring Environmental Degradation in the Nilgiri Biosphere Reserve and Its Ecosystem of Western Ghats, India. *ISPRS Int. Arch. Photogramm. Remote Sens. Spat. Inf. Sci.* **2020**, *XLIII-B3-2*, 933–940. [\[CrossRef\]](#)
59. Rhee, J.; Im, J.; Carbone, G.J. Monitoring agricultural drought for arid and humid regions using multi-sensor remote sensing data. *Remote Sens. Environ.* **2010**, *114*, 2875–2887. [\[CrossRef\]](#)
60. Zhang, L.; Jiao, W.; Zhang, H.; Huang, C.; Tong, Q. Remote Sensing of Environment Studying drought phenomena in the Continental United States in 2011 and 2012 using various drought indices. *Remote Sens. Environ.* **2017**, *190*, 96–106. [\[CrossRef\]](#)
61. Cao, Y.; Chen, S.; Wang, L.; Zhu, B.; Lu, T.; Yu, Y. An Agricultural Drought Index for Assessing Droughts Using a Water Balance Method: A Case Study in Jilin Province, Northeast China. *Remote Sens.* **2019**, *11*, 1066. [\[CrossRef\]](#)
62. Bhuiyan, C. Various drought indices for monitoring drought condition in Aravalli terrain of India. In Proceedings of the XXth ISPRS Conference 2004, Istanbul, Turkey, 12–23 July 2014; pp. 907–912.
63. Brown, J.F.; Wardlow, B.D.; Tadesse, T.; Hayes, M.J.; Reed, B.C. The Vegetation Drought Response Index (VegDRI): A New Integrated Approach for Monitoring Drought Stress in Vegetation. *GIScience Remote Sens.* **2008**, *45*, 16–46. [\[CrossRef\]](#)
64. Tadesse, T.; Wardlow, B.D.; Hayes, M.J.; Svoboda, M.D.; Brown, J.F. The Vegetation Outlook (VegOut): A New Method for Predicting Vegetation Seasonal Greenness. *GIScience Remote Sens.* **2010**, *47*, 25–52. [\[CrossRef\]](#)

65. Heim, R.R., Jr. A review of twentieth-century drought indices used in the United States. *Bull. Am. Meteorol. Soc.* **2002**, *83*, 1149–1165. [[CrossRef](#)]
66. Johnson, D.P.; Stanforth, A.; Lulla, V.; Luber, G. Developing an applied extreme heat vulnerability index utilizing socioeconomic and environmental data. *Appl. Geogr.* **2012**, *35*, 23–31. [[CrossRef](#)]
67. Balasubramani, K.; Leo George, S.; Anusuya, K.; Venkatesh, R.; Thilagaraj, P.; Gnanappazham, L.; Kumaraswamy, K.; Balasundareswaran, A.; Praveen, B. Revealing the socio-economic vulnerability and multi-hazard risks at micro-administrative units in the coastal plains of Tamil Nadu, India. *Geomat. Nat. Hazards Risk* **2021**, *12*, 605–630. [[CrossRef](#)]
68. Murthy, C.S.; Singh, J.; Kumar, P.; Sesha Sai, M.V.R. Meteorological drought analysis over India using analytical framework on CPC rainfall time series. *Nat. Hazards* **2016**, *81*, 573–587. [[CrossRef](#)]
69. Guhathakurta, P.; Menon, P.; Inkane, P.M.; Krishnan, U.; Sable, S.T. Trends and variability of meteorological drought over the districts of India using standardized precipitation index. *J. Earth Syst. Sci.* **2017**, *126*, 120. [[CrossRef](#)]
70. Dhiman, S.C. Rejuvenation of Aquifers. In *Water Governance: Challenges and Prospects*; Springer: Berlin/Heidelberg, Germany, 2019; pp. 187–204. [[CrossRef](#)]
71. Chandrasekar, K.; Sesha Sai, M.V.R.; Roy, P.S.; Jayaraman, V.; Krishnamoorthy, R. Identification of Agricultural Drought Vulnerable Areas of Tamil Nadu, India Using Gis-Based Multi Criteria Analysis. *Asian J. Environ. Disaster. Manag.* **2014**, *1*, 40–61. [[CrossRef](#)]
72. Varadan, R.J.; Kumar, P. Mapping agricultural vulnerability of Tamil Nadu, India to climate change: A dynamic approach to take forward the vulnerability assessment methodology. *Clim. Change* **2015**, *129*, 159–181. [[CrossRef](#)]
73. Vaani, N.; Porchelvan, P. Monitoring of agricultural drought using fortnightly variation of vegetation condition index (VCI) for the state of Tamil Nadu, India. *Int. Arch. Photogramm. Remote Sens. Spat. Inf. Sci. ISPRS Arch.* **2018**, *42*, 159–164. [[CrossRef](#)]
74. Balasundareswaran, A.; Kumaraswamy, K.; Balasubramani, K. Multi-Hazard Zonation For Effective Management of Disasters in Tamil Nadu. *Geosfera Indones.* **2020**, *5*, 65–79. [[CrossRef](#)]
75. Das, P.K.; Das, R.; Das, D.K.; Midya, S.K.; Bandyopadhyay, S.; Raj, U. Quantification of agricultural drought over Indian region: A multivariate phenology-based approach. *Nat. Hazards* **2020**, *101*, 255–274. [[CrossRef](#)]
76. Vengateswari, M.; Geethalakshmi, V.; Bhuvaneswari, K.; Jagannathan, R.; Panneerselvam, S. District level drought assessment over Tamil Nadu. *Madras Agric. J.* **2019**, *106*, 2016–2018. [[CrossRef](#)]
77. Balaganesh, G.; Malhotra, R.; Sendhil, R.; Sirohi, S.; Maiti, S.; Ponnusamy, K.; Sharma, A.K. Development of composite vulnerability index and district level mapping of climate change induced drought in Tamil Nadu, India. *Ecol. Indic.* **2020**, *113*, 106197. [[CrossRef](#)]
78. Arulnagai, R.; Mohamed Sihabudeen, M.; Vivekanand, P.A.; Kamaraj, P. Influence of physico chemical parameters on potability of ground water in ariyalur area of Tamil Nadu, India. *Mater. Today Proc.* **2020**, *24*, 923–928. [[CrossRef](#)]